Molecular Simulation Study of the Potentials of Mean Force for the Interactions between Models of Like-Charged and between Charged and Nonpolar Amino Acid Side Chains in Water

Katarzyna Maksimiak,[†] Sylwia Rodziewicz-Motowidło,[†] Cezary Czaplewski,[†,‡] Adam Liwo,[†,‡,§] and Harold A. Scheraga*[,‡]

Faculty of Chemistry, University of Gdansk, Sobieskiego 18, 80-952 Gdansk, Poland, Baker Laboratory of Chemistry and Chemical Biology, Cornell University, Ithaca, New York, 14853-1301, and Academic Computer Center in Gdansk TASK, Technical University of Gdansk, Narutowicza 11/12, 80-952 Gdansk, Poland

Received: May 30, 2003

The purpose of this study was to determine the potentials of mean force (PMF) of the interactions between models of like-charged and between models of charged and nonpolar amino acid side chains in water to design improved side chain−side chain interaction potentials for our united residue UNRES force field for protein-structure prediction. Restrained molecular dynamics with the AMBER force field, the TIP3P model of water, and the Ewald summation were used to carry out simulations, and the weighted histogram analysis method (WHAM) was used to calculate the PMFs as functions of solute−solute distances. The following types of systems were considered to model the interactions between like-charged side chains and the interactions between charged and nonpolar side chains: (i) a pair of positively charged ions (potassium, ammonium, and guanidine, respectively); (ii) a pair of negatively charged ions (chloride and acetate, respectively), and (iii) pairs of methane with potassium, ammonium, and chloride ions, respectively. Additionally, a pair of potassium and chloride ions was included for comparison with the work of other authors. Except for the pair of acetate ions, where the PMF curve exhibited all-repulsive behavior, a minimum or two coalescing minima with positive PMF values appeared for pairs of like-charged ions. In the potassium−chloride ion pair, a contact and a solvent-separated minimum was observed. Comparison of our results with those obtained by other authors showed that including Ewald summation in computing electrostatic interactions has substantial influence on the PMFs of like-charged ions; for oppositely charged ions including Ewald summation only causes deepening of the contact minimum. It was found that the appearance of the minimum in the PMFs of like-charged ion pairs is caused by a high degree of ordering of water molecules and counterions between the solutes at this distance. The solvent contribution to the PMFs of pairs of charged and nonpolar solutes is positive in all cases; the most unfavorable contribution was observed for the methane−chloride ion pair. The results demonstrate that the use of all-repulsive potentials for the interactions between like-charged and between charged and nonpolar side chains in the UNRES force field is essentially correct, but the distance dependence should be more long range in the like-charged side chain interaction potential, because the PMF curves of like-charged ion pairs are reasonably fitted with a combination of r^{-1}, r^{-2}, and r^{-3} terms (r being the distance between the centers of the mass), while they are not reproduced well with combinations of r^{-6} and r^{-12} terms of the present version of UNRES.

Introduction

The interaction with water is one of the principal factors determining the spatial structure of proteins and other biomolecules by forcing polar groups to the surface and nonpolar ones to form a hydrophobic core.[1−9] Therefore, accurate modeling of these interactions is necessary for the construction of force fields for biomolecular simulations. In the past few years, we have developed a united residue force field, hereafter referred to as UNRES,[10−12] in which two types of interaction sites are distinguished, namely, peptide groups (p) and side chains (SC), as shown in Figure 1. The energy of the virtual bond chain consists of the energy of interaction between side chain centers ($U_{SC_iSC_j}$), between side chain centers and the peptide groups ($U_{SC_ip_j}$), between peptide groups (U_{pp}), as well as of torsional (U_{tor}), double-torsional (U_{tord}), virtual-bond-angle bending (U_b), side chain rotamer (U_{rot}), and multibody or correlation (U_{corr}) components, as given by eq 1.

$$U = \sum_{i<j} U_{SC_iSC_j} + w_{SCp}\sum_{i\neq j} U_{SC_ip_j} + w_{el}\sum_{i<j-1} U_{p_ip_j} + w_{tor}\sum_i U_{tor}(\gamma_i) + w_{tord}\sum_i U_{tord}(\gamma_i,\gamma_{i+1}) + w_b\sum_i U_b(\theta_i) + w_{rot}\sum_i U_{rot}(\alpha_{SC_i},\beta_{SC_i}) + \sum_{m=2}^{N_{corr}} w^{(m)}_{corr} U^{(m)}_{corr} \quad (1)$$

$U_{SC_iSC_j}$ is the potential of mean force (PMF) of the interaction between side chains SC_i and SC_j in water; in this regard, it describes hydrophobic/hydrophilic interactions. In the present version of UNRES, two types of interaction potentials are used: (i) a Lennard-Jones form for interactions between

* Corresponding author. Phone: (607) 255-4034; fax: (607) 254-4700; e-mail: has5@cornell.edu.
[†] University of Gdansk.
[‡] Cornell University.
[§] Technical University of Gdansk.

10.1021/jp030691w CCC: $25.00
Published on Web 11/11/2003

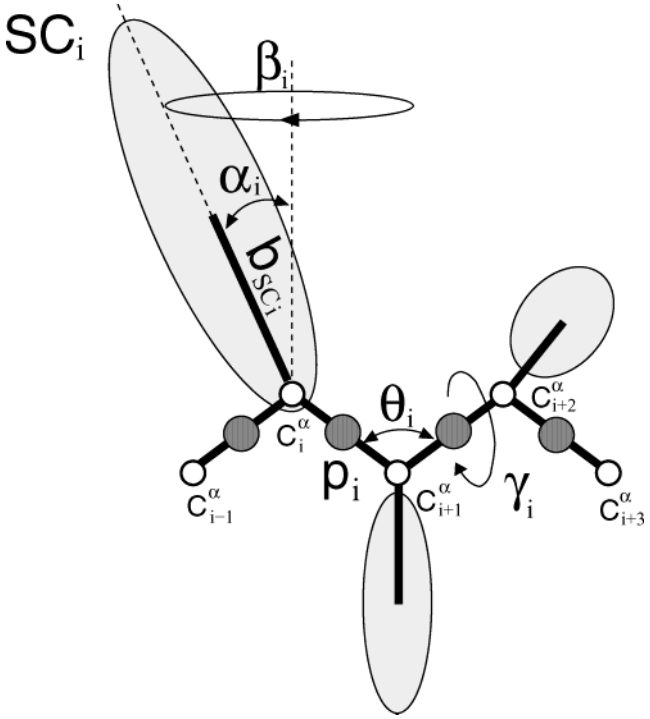

Figure 1. The UNRES model of polypeptide chains. The interaction sites are side chain ellipsoids of different sizes (SC) and peptide-bond centers (p) indicated by shaded circles, whereas the α-carbon atoms (small empty circles) are introduced to define the backbone local interaction sites and to assist in defining the geometry.

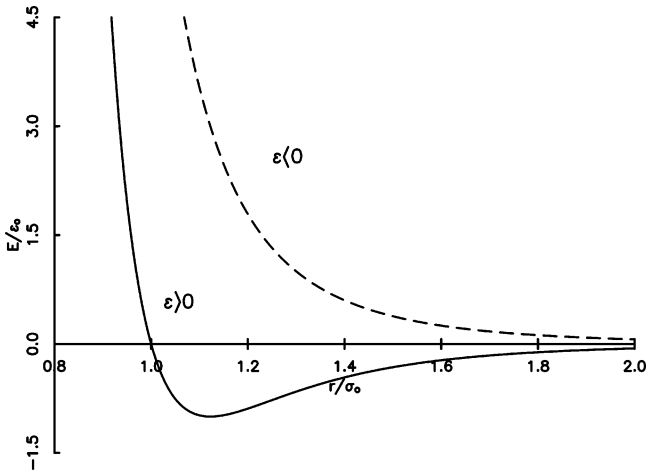

Figure 2. Illustration of the distance dependence of the side chain interaction potential of UNRES for attractive-and-repulsive ($\epsilon > 0$) and all-repulsive ($\epsilon < 0$) interactions.

nonpolar side chains or between side chains bearing opposite charges and (ii) an all-repulsive Lennard-Jones-like potential for interactions between hydrophilic side chains bearing either the same charge or no charge, or if only one of them is charged,[13] as given by eq 2 and illustrated in Figure 2.

$$U_{SC_iSC_j} = 4|\epsilon_{ij}|\left(\frac{\sigma}{r}\right)^{12} - 4\epsilon_{ij}\left(\frac{\sigma}{r}\right)^{6} \qquad (2)$$

These functional forms were chosen only because of their simplicity and computational efficiency. We have recently begun a series of molecular-simulation studies aimed at designing more accurate forms of the potential of mean force. Recently,[14−16] we carried out molecular dynamics (MD) studies of two- and multibody potentials of mean force for the hydrophobic interaction between nonpolar solutes in water. The aim of the work reported here was to extend the MD simulations to pairs of charged amino acid side chains and pairs composed of charged and uncharged side chains.

Several studies have been carried out to determine the PMF of pairs of simple like-charged ions, such as lithium, sodium, potassium, and chloride as well as pairs of simple oppositely charged ions.[17−30] The PMF was determined both by molecular simulations[18,20,22,23,25,26,29,30] and by solving integral equations.[17,19,21,24,27,28] Although the results differ depending on the approach and water model used, the PMFs of like-charged ion pairs exhibit one or two minima corresponding to the favorable interactions with intervening water molecules.[22,27,28] The PMFs of oppositely charged ion pairs exhibit a deep contact minimum and a shallower solvent-separated minimum.[22,26] Studies have also been carried out on the PMF of the guanidine−guanidine,[31] lysine−lysine,[32] and guanidine−acetate,[33] ion pair in water to model charge−charge interactions in proteins. A study of the PMF of chloride−argon and sodium−argon pairs in water modeling the charged-nonpolar side chain pairs was carried out by Gaigeot and Borgis.[34]

Recently, a large-scale umbrella-sampling MD study of the PMF of the pairs of all charged and polar side chains in proteins was carried out by Masunov and Lazaridis.[29] These authors used a spherical cluster of 200 water molecules immersed in continuous dielectric to simulate the solvent; no periodic boundary conditions were implemented. However, they studied full side chains in extended conformations and it is, therefore, difficult to capture effects arising from the interactions between the charged parts of the side chains and between the charged and noncharged parts. Moreover, the accuracy of the PMF decreases with the size and complexity of the solute molecules. Therefore, in this study we decided to use simple models of charged and nonpolar side chains.

Methods

The following systems have been considered:

(i) a pair of potassium, a pair of ammonium, and a pair of guanidine ions, which model the interactions within a pair of amino acid side chains bearing equally charged groups such as, for example, the side chain of the amino group of lysine or ornithine.

(ii) a pair of chloride ions and a pair of acetate ions, which model the interactions between negatively charged side chains, such as aspartate and glutamate.

(iii) a pair consisting of a methane molecule and a potassium ion or an ammonium ion, which model the interactions between nonpolar and charged side chains.

The purpose of using both simple ions (potassium and chloride) and ions modeling the charged parts of the side chains of amino acids was to determine the influence of the presence of hydrogen-bond donor or acceptor groups in solute molecules on the PMF. For comparison of the results of our simulations with the work of other authors, we also carried out calculations on a pair consisting of the potassium and the chloride ions. To some extent, this pair could be regarded as a model for the interactions within a pair of oppositely charged side chain groups such as, for example, the amino group of lysine and the carboxylate group of aspartic acid; however, we leave the problem of interactions between oppositely charged side chains to a further detailed study.

In all cases, the distance between the geometric centers of the solute particles was the reaction coordinate.

The potential of mean force (PMF), $W(r)$, of a pair of solute molecules in water separated by a distance r is defined by eq 3.

$$W(r) = -RT \ln P(r,p,T,V) \tag{3}$$

where $P(r)$ is the conditional probability density of the variables of interest at a given value of r; p, T, and V are the pressure, temperature, and volume of the system, and

$$P(r,p,T,V) = \frac{\int_{V_r} \exp(-H(\mathbf{x}))\, dV}{\int_{V} \exp(-H(\mathbf{x}))\, dV} \tag{4}$$

where H is the Hamiltonian of the system (solute plus solvent with coordinates $\mathbf{x}$), V is the volume of the whole configurational space of the system, and V_r is the volume of the fraction of the configurational space restricted to r.

To determine the PMF by molecular simulations, the umbrella-sampling method was used.[35,36] A series of restraining potentials, V, was imposed on the reaction coordinate to ensure that all regions are sampled sufficiently. Each restraint defined a sampling window. The total Hamiltonian of the system (including the restraining potential) for the ith window was defined by

$$H_i(r) = V_o(r) + V_i(r) = V_o(r) + \frac{1}{2}K_i(r - r^{o}_i)^2 \tag{5}$$

where V_o is the energy function of the system consisting of the solute and the solvent, K_i and r^{o}_i are the force constant and the equilibrium distance of the restraining potential, respectively, with the assumption that $K = 2$ kcal/Å^2. A total of 12 windows with r° varying from 3.0 to 8.5 Å was used. To calculate the PMF from umbrella-sampling simulation data, the weighted histogram analysis method (WHAM)[37,38] was used, as in our previous study of the hydrophobic association of methane.[14] This method processes the results of simulations from all windows simultaneously and removes the contribution arising from the restraining potential V.

The sampling was carried out by means of MD calculations in the NVT ensemble, with the AMBER[39,40] force field and the TIP3P model of water.[41,42] The calculations were carried out by using a cubic periodic box with a 20 Å side. For simple ion pairs (the potassium−potassium, chloride−chloride, and the potassium−chloride pair), a cutoff of 9.9 Å for the nonbonded interactions was applied in the production simulations; this cutoff was slightly less than a half of box dimension, which assured that the miminum image convention was satisfied. For other systems, a cutoff of 9.0 Å on nonbonded interactions was applied. The electrostatic energy was evaluated using the particle-mesh Ewald summation,[43] and counterions (sodium, if the solute was negatively charged or chloride, if the solute was positively charged) were added to the systems to zero the net charge. For all simulations except the methane−potassium cation and methane−ammonium cation pair, where more subtle effects were to be observed, the duration of the simulation in each window was 1 ns and the sampling frequency was 2 fs, which gave a total of 500 000 data points in each window. For the methane−potassium cation and methane−ammonium cation pairs, the duration was 1.98 ns, which gave a total of 990 000 data points in each window.

The methane molecule was modeled by a single interaction site (i.e., a united CH_4 atom) with parameters of the Lennard-Jones potential determined by Jorgensen et al.[44] The methyl group of the acetate anion was considered as a single interaction site, the van der Waals (VDW) parameters being taken from the AMBER 84 united atom force field.[45] Partial atomic charges on the atoms of the ammonium and guanidine cations as well as on the acetate anion were computed by fitting the point-charge electrostatic potential to the molecular electrostatic potential computed using the electronic wave function calculated at the restricted Hartree−Fock (RHF) level with the 6-31G* basis set. The program GAMESS[46] was used to carry out quantum-mechanical calculations, while the program RESP[47] of the AMBER 5.0 package was used to compute the fitted charges. The charges are shown in Figure 3. Except for the K^+−C4 pair, all the pairwise VDW parameters were generated from single-atom parameters by using the Lorentz−Berthelot mixing rules.[48]

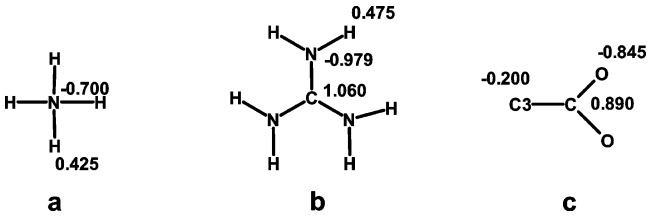

Figure 3. Partial atomic charges (in electron charge units) on the atoms of the ammonium cation (a), guanidine cation (b), and acetate anion (c). The AMBER types of the respective atoms are also indicated.

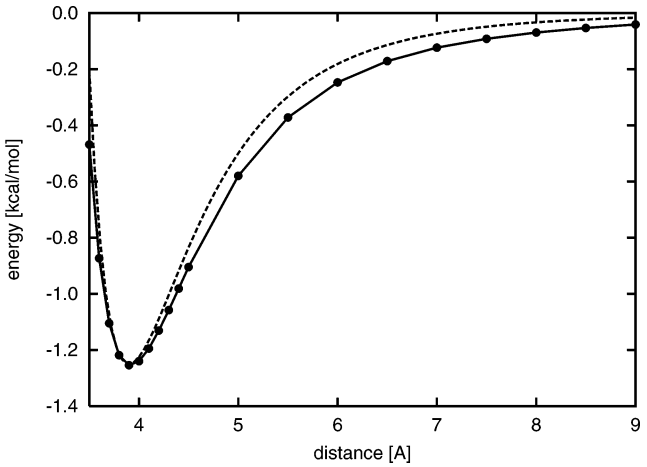

Figure 4. RHF/6-31G** ab initio energies (circles) and the fitted Lennard-Jones potential curve (dashed line) of the methane−K^+ pair as a function of the distance between the carbon and potassium atom.

$$\sigma_{ij} = (\sigma_{ii} + \sigma_{jj})/2 \tag{6}$$

$$\epsilon_{ij} = \sqrt{\epsilon_{ii}\epsilon_{jj}} \tag{7}$$

where i,j are two different types of atoms and σ and ϵ correspond to the VDW parameters associated with the contact distance and the depth of the well, respectively.

The VDW parameters of the C4 (methane)−K^+ pair were determined separately. It has been demonstrated in an earlier work that the interaction potential of the sodium cations with nonpolar closed-shell argon atoms (i.e., between a charged and a nonpolar system) contains a pronounced minimum.[34] Because the VDW parameters of the potassium cations used in the AMBER force field[49] derived to reproduce the cation hydration energies correspond to a very shallow potential well, we decided to use ab initio RHF/6-31G** calculations of the methane−potassium cation system to derive the interaction potential. The energy of the system was evaluated from 3.5 to 9 Å with a grid of 0.5 Å for most of the points and 0.1 Å in the region of the

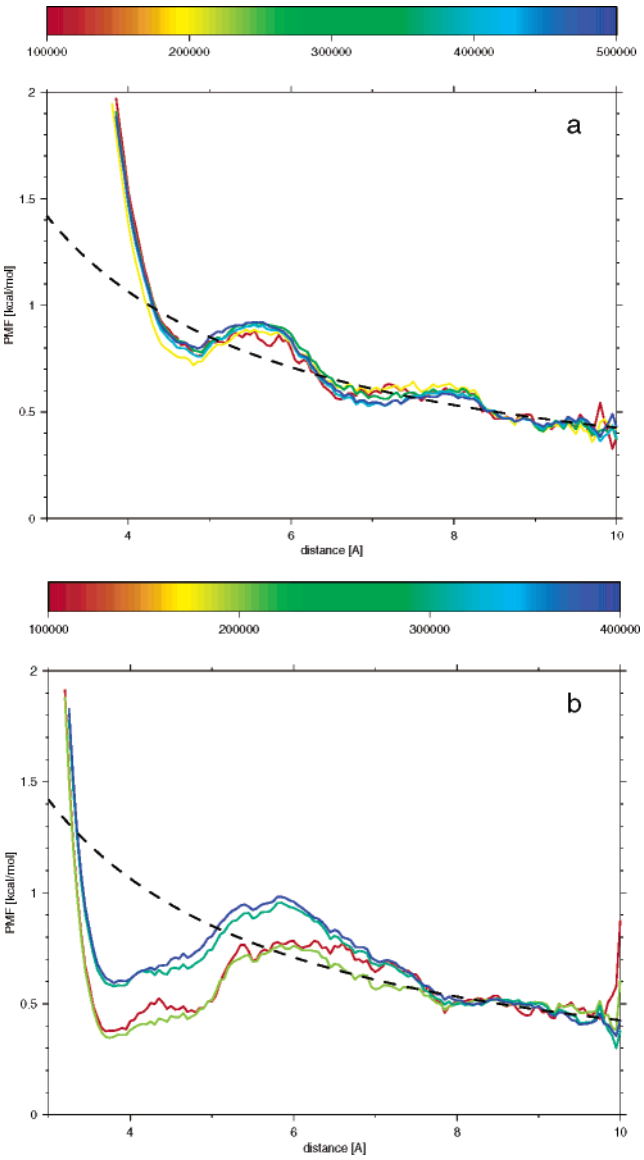

Figure 5. Convergence plots of the PMF of the ammonium−ammonium system (a) and the guanidine−guanidine system (b). Curves are color-coded depending on the number of simulation points taken.

minimum of the energy (from 3.5 to 4.5 Å). Because the methane molecule has high symmetry, we chose one relative orientation of the interacting species, in which the potassium cation approached the methane molecule along the bisector of one of the H−C−H valence angles (i.e., along a S_4 improper-rotation axis). The basis set superposition error (BSSE) was estimated at each point by using the counterpoise Boys−Bernardi method.[50] As shown in Figure 4, the interaction-energy curve is well approximated by a Lennard-Jones curve with $\epsilon = 1.25$ kcal/mol and $r° = 3.9$ Å (i.e., with the same minimum-energy value and minimum distance as the ab initio curve); these parameters were used in the MD simulations of the potassium ion−methane pair.

All other force field parameters (bond and bond angle parameters and VDW parameters) were taken directly from the AMBER 5.0 force field.[39,40]

Results and Discussion

Sample plots, showing how the convergence of the PMF depends on the number of data points taken for the pair of the ammonium and the guanidine cations, respectively, are shown in Figure 5. It can be seen that the convergence is very rapid for small nearly spherical ammonium cations and still acceptable for large nonspherical guanidine cations.

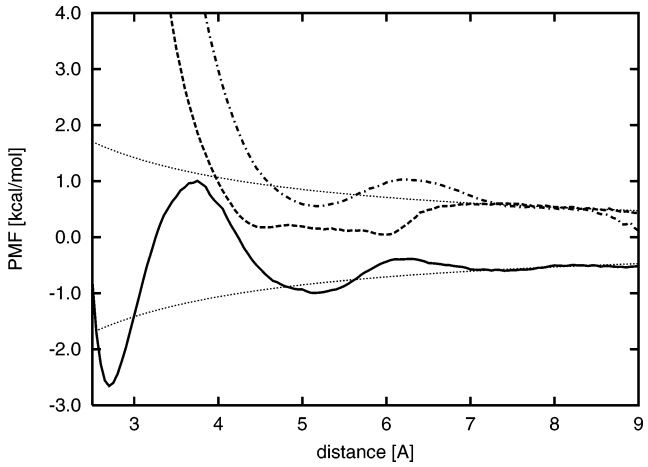

Figure 6. The PMFs for a pair of potassium (dashed line), chloride (dot−dashed line), and a pair composed of a potassium and a chloride ion (solid line) in water as a function of solute−solute distance. The thin dotted lines are the anticipated long-range Coulomb distance dependence curves of the PMF of the interaction of ions with equal and opposite charge, respectively.

Figure 6 compares the PMFs of a pair of potassium ions, a pair of chloride ions, and a pair composed of a potassium and a chloride ion. The PMFs of pairs of equally charged ions contain a minimum or a region of two coalescing minima centered at about 5 Å. There are two minima in the PMF of the potassium−chloride system: one at 2.7 Å, which is a contact minimum and another one at 5.0 Å, as in the case of pairs of equally charged ions. It can be seen that, in all three cases, the PMF obeys the Coulomb law at large distances, with the dielectric constant of water, ϵ, of 78; this was taken as the reference PMF at large distances.

The PMF curve of the K^+-Cl^- pair is similar to the curve reported by Masunov and Lazaridis,[29] although a different simulation protocol and force field was used. The contact minimum in the latter work[29] appears at 3.1 Å and the solvent-separated minimum appears at 5.4 Å, their depths being about −1.8 kcal/mol and −1 kcal/mol, respectively. Thus, the contact minimum in our work appears at a shorter distance and is deeper by about 1 kcal/mol compared to that in ref 29. It can be supposed that the difference between the depth of the contact minimum found in our and Masunov and Lazaridis work is caused by the fact that the other authors did not use the Ewald summation. They reported that, for the Na^+-Cl^- pair, the use of the Ewald summation deepened the PMF curve by about 1 kcal/mol compared to the PMF curve obtained by using the spherical cluster of 200 water molecules (Figure 2 in ref 29).

The PMF curves of simple like-charged ions obtained in this work differ from those obtained by Masunov and Lazaridis.[29] The minimum of the PMF curve for the $Cl^-−Cl^-$ pair obtained in their work has a negative PMF value, which is lower than that of the $K^+−K^+$ pair. The PMF curve of the $Cl^-−Cl^-$ pair resulting from our calculations is above that of the $K^+−K^+$ pair (Figure 6). On the other hand, our $Cl^-−Cl^-$ PMF curve agrees well (both in the positions and in the PMF values of the maxima and minima) with those obtained with MD simulations by Guàrdia et al.,[22] and Shinto et al.,[30] carried out with different potentials to describe the VDW interactions between solute particles, the SPC and not the TIP3P water model and using integration of the mean force and not the WHAM method to

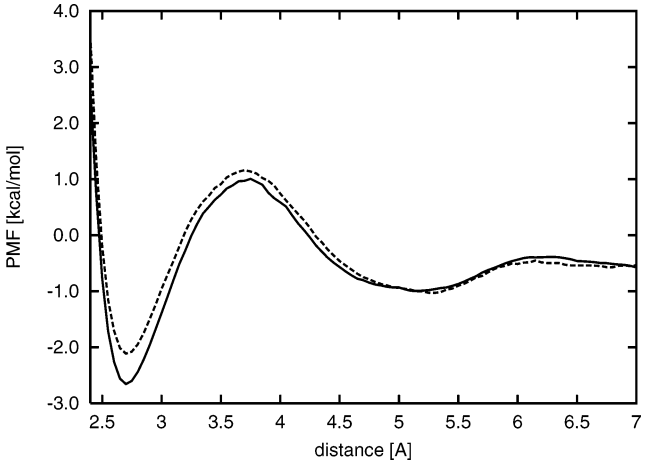

Figure 7. Comparison of the PMF curves for the K^+-Cl^- pair in water obtained with the Ewald summation (solid line) and with a 9 Å spherical cutoff (dashed line) in computing the electrostatic interaction energy. The curve is shown until 7 Å distance because artifacts due to using a spherical cutoff appear beyond that distance.

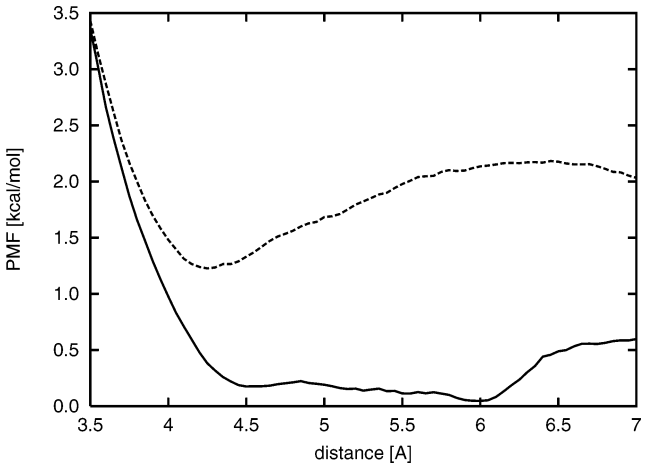

Figure 8. Comparison of the PMF curves for the K^+-K^+ pair in water obtained with the Ewald summation (solid line) and with a 9 Å spherical cutoff (dashed line) in computing the electrostatic interaction energy. The curve is shown until 7 Å distance because artifacts due to using a spherical cutoff appear beyond that distance.

derive the PMF. In both cases, the Ewald summation was used to compute electrostatic interactions.[22,30] Our PMF curve also agrees qualitatively with those obtained by other authors.[18,19,24,25,51]

To determine whether the difference between our results and those of Masunov and Lazaridis could be a result of their use of a finite simulation sphere, we carried out supplementary MD simulations of the K^+-Cl^- and K^+-K^+ pair with a spherical 9.9 Å distance cutoff applied both to the nonbonded and to the electrostatic interactions. The resulting PMF curves are compared with the curves obtained from the simulations with the Ewald summation in Figures 7 and 8. It can be seen that the contact minimum of the K^+-Cl^- pair is depleted by almost 1 kcal/mol, while the curves between 3 and 7 Å overlap well. On the another hand, the PMF curves of the K^+-K^+ pair are different, the minimum being shifted to 4.3 Å by use of the 9.9 Å spherical cutoff instead of Ewald summation to compute electrostatic interactions. Therefore, the difference between the PMF curves obtained in our work and those of Masunov and Lazaridis[29] can be attributed to the fact that the Ewald summation was used in our simulations.

Our PMF curve obtained for the Cl^-Cl^- ion pair is qualitatively similar to the PMF curves obtained recently by Kovalenko and Hirata[27,28] by using the variations of the dielectrically corrected RISM/HNC (DRISM/HNC) theory, the difference being that this theory predicts the minimum in the PMF at about 4 Å and not 5 Å. Earlier applications of the RISM theory[17] predicted the minimum at less than 4 Å with negative PMF value.

To understand the origin of the minima in the PMFs of like-charged ion pairs, we analyzed the distribution of counterions and water molecules around the interacting pair. Two-dimensional plots of the counterion and water-molecule distributions around the solutes for the potassium-pair and chloride-pair system for intersolute distances corresponding to energy minima are shown in Figures 9 and 10, respectively. It can be seen that, for both ion pairs, the counterions tend to be located near the intersection of the molecular surfaces of the solute particles. Additionally, for the pair of potassium ions there is high water density near the intersection of the molecular surfaces of the solute particles. The locally enhanced concentration of counterions and solvent molecules can provide enhanced screening of repulsive electrostatic interactions which, in turn, could explain the presence of a minimum in the PMF of the potassium-ion pairs, although the ions bear the same charge. Bridging a like-charged ion pair by water molecules was proposed as the explanation for the appearance of minima in the PMF by Guàrdia et al.[22] and by Kovalenko and Hirata.[28]

Figure 11 shows the PMFs of the ammonium ion pair (model of lysine side chains) and guanidine ion pair (model of arginine side chains) in water compared with the PMF of two potassium ions. Figure 12 shows the PMF of a pair of acetate ions in water compared to that of the chloride-ion pair. It can be seen that these PMF curves (which correspond to more realistic models of charged side chains) are remarkably different from the curves obtained for the pairs of simple ions in water. The minima become shallower or even disappear in the acetate-pair system. This can be attributed to the tendency to form strong hydrogen bonds with water molecules; therefore, bridging of two ions by a water molecule or by a counterion is less favorable than full solvation of these ions. It can also be seen that the minimum of the PMF of the guanidine-ion pair (Figure 11) is remarkably deeper compared to that of the ammonium-ion pair (Figure 11). This can be attributed to the tendency of charged guanidine groups to form water-bridged structures[52] (e.g., there are many more pairs of arginine residues at a contact distance in the PDB compared to the number of lysine pairs[13]).

As in the case of simple ions, the PMF curves of the three pairs mentioned above are different from the PMF curves of the same or analogous systems studied by Masunov and Lazaridis.[29] These authors obtained a pronounced energy minimum for the Lys^+-Lys^+ pair at about 5 Å, the minimum value of the PMF being negative (Figure 16 in ref 29). In this case, we can compare the results of our and their simulations directly, because the ammonium groups of charged lysine side chains in their study were constrained to face each other. Such configuration leads to interactions very similar to those between two unconstrained ammonium groups. Likewise, there are two pronounced minima in their PMF curves of arginine side chains corresponding to face-to-face and stacking arrangements of guanidine groups of charged arginine side chains (Figure 6 in ref 29), while our PMF curves of guanidine cation pair exhibits only a contact minimum with a positive PMF value (Figure 11). Their PMF curve of a pair of acetate ions in carboxyl-to-carboxyl orientation exhibits a pronounced contact minimum with a negative PMF value at 3.6 Å, while there are no minima in our PMF curve for the acetate pair (Figure 12). Although

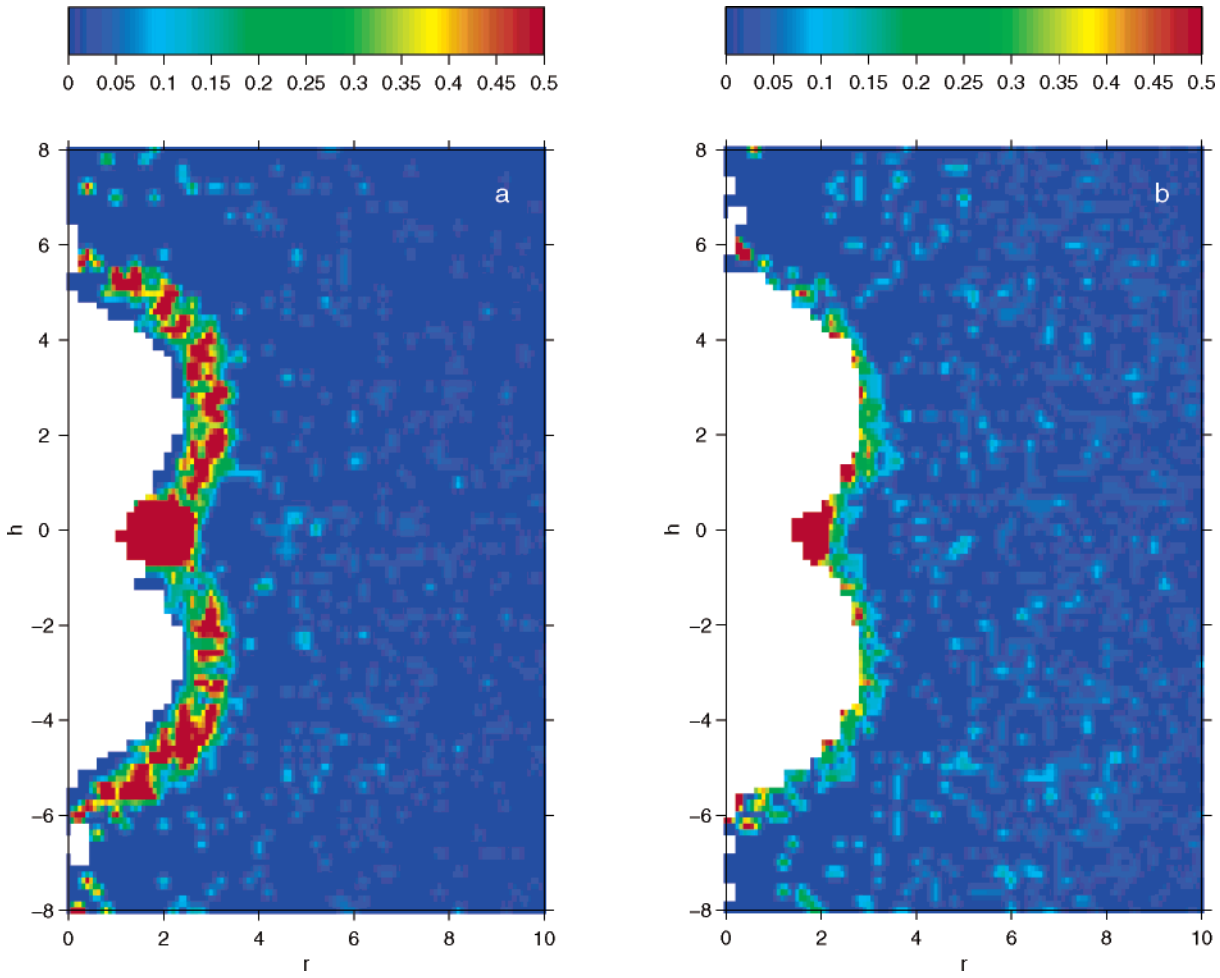

Figure 9. Normalized number density of counterions per unit volume around a pair of potassium (a) and chloride (b) ions in water. The plots are made in plane containing the K^+-K^+ or the Cl^--Cl^- axis, resepectively. *h* is the coordinate along the axis, while *r* is the coordinate lying in the plane and perpendicular to the axis. The molecular surfaces of the ions intersect at a circle lying in the plane perpendicular to the plane of the drawing and containing the line $h = 0$.

our results for the last two pairs cannot be compared directly with those of Masunov and Lazaridis, because our PMFs are averaged over all possible orientations, in view of the differences between their and our PMF curves for simple like-charged ions, it can be concluded that the differences arise mainly because Masunov and Lazaridis did not use Ewald summation.

The PMF curves for the pairs composed of a methane molecule and a potassium, ammonium, or a chloride ion, respectively, are shown in Figure 13 in comparison with the PMF of two methane molecules in water [taken from our earlier work[14] and corresponding to calculations using the Ewald summation (Figure 5 in ref 14)]. The PMF of the methane−potassium cation pair has a contact minimum at 4.1 Å with a PMF value of −0.65 kcal/mol. However, in view of the fact that the Lennard-Jones potential derived in this work (Figure 4) has a minimum with energy −1.25 kcal/mol, it can be concluded that the reaction field works toward diminishing the interaction between the potassium cation and the methane molecule. This is clearly visualized in Figure 14, in which the solvent contributions to the PMFs for methane−methane, methane−potassium ion, and methane−chloride ion pairs are summarized. The PMF curve for the methane−ammonium cation pair in Figure 13 contains a less pronounced minimum and the PMF curve for the methane−chloride ion pair contains only a solvent-separated minimum at about 7 Å. The differences between the PMF curves for the methane−potassium and the methane−chloride ion pair are better seen in the solvent-contribution curves (Figure 14); the curve for the methane−potassium ion pair is steadily decreasing with distance, while that of the methane−chloride ion pair exhibits a maximum analogous to the cavity-creation maximum in the PMF curves for hydrophobic solutes. Similar differences between the solvent contributions to the PMF for argon−sodium ion and argon−chloride ion pairs were reported by Gaigeot et al.[34] It can, therefore, be concluded that the PMFs for pairs of charged and nonpolar side chains are characteristic of a repulsive potential, which is in agreement with the fact that the contact energies of pairs of hydrophobic and hydrophilic amino acid residues determined from the PDB statistics are positive.[13]

In view of the fact that the interaction potential of charged−uncharged particle pairs turned out to be substantially more attractive than that derived from standard force field parameters (see Methods), concern can be raised as to how sensitive the PMFs for charged−nonpolar solute pairs are to the parameters of the interaction potential. Figure 15 compares the total PMF and solvent contributions to the PMF curves for the methane−potassium ion pair obtained with the Lennard-Jones potential parameters derived in this work from ab initio calculations and those obtained by Åqvist.[49] It can be seen that, while the total PMF curves are different, the solvent-contribution curves are almost identical.

The potentials of interaction between like-charged and between charged and nonpolar side chains used in UNRES are all-repulsive analogues of the Lennard-Jones potential (eq 2)

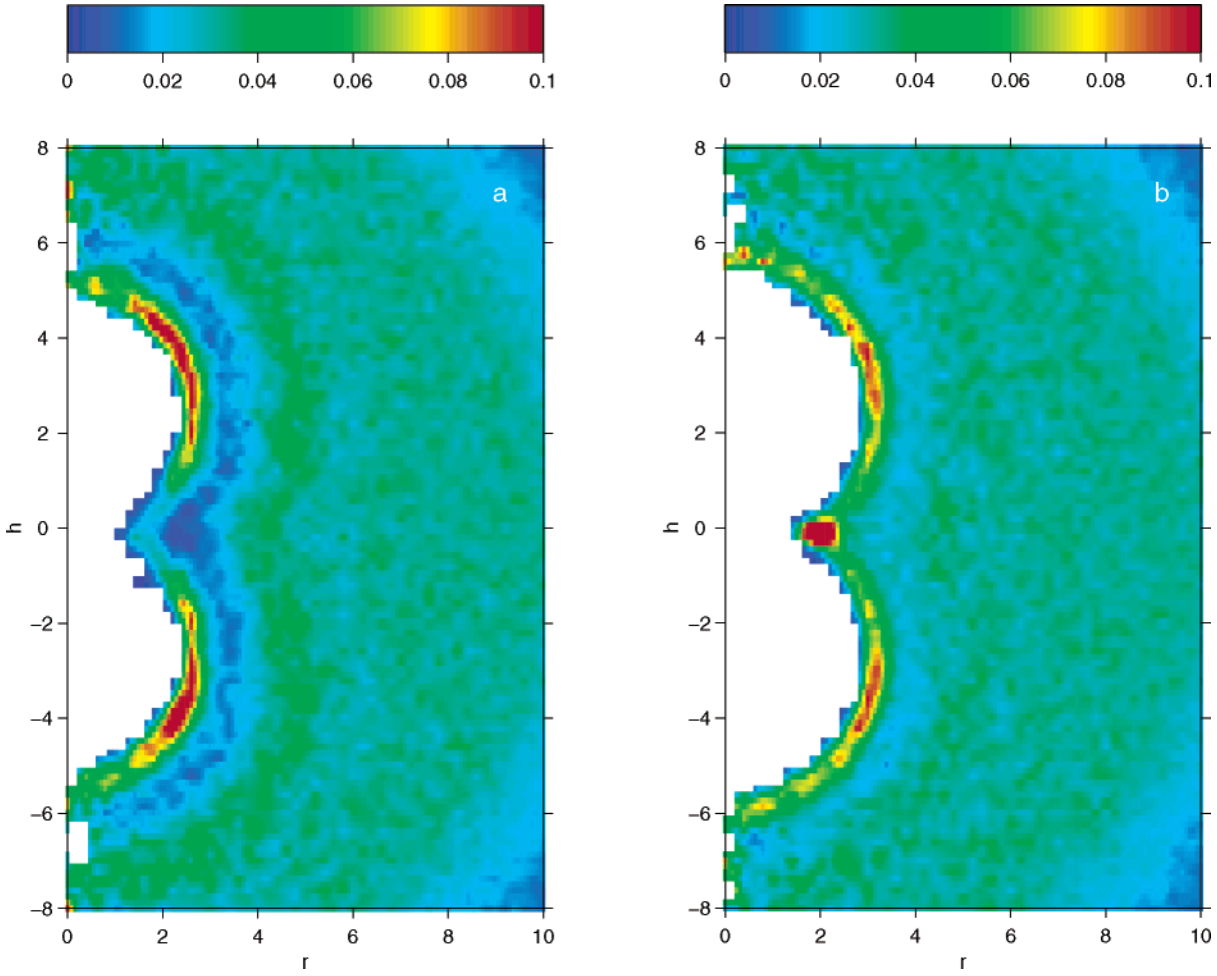

Figure 10. Normalized number density of water molecules per unit volume around a pair of potassium (a) and chloride (b) ions in water.

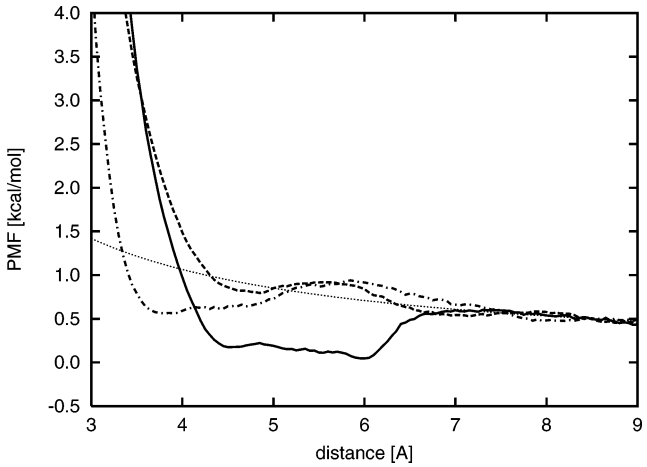

Figure 11. PMF curves for a pair for potassium (solid line), ammonium (dashed line), and guanidine (dot−dashed line) ions in water. The thin dotted line is the anticipated long-range Coulomb distance dependence curve of the PMF.

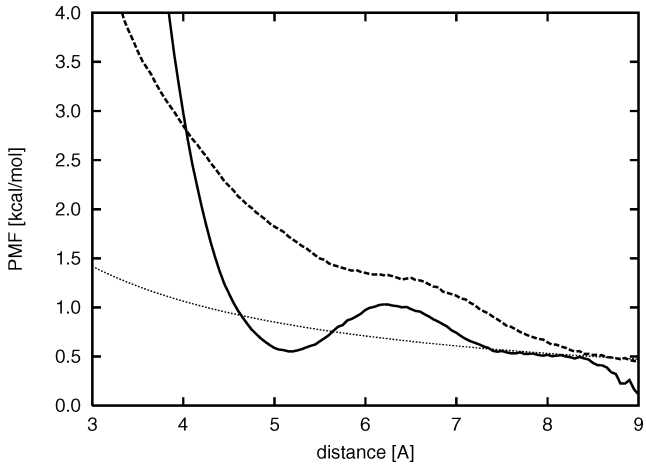

Figure 12. PMF curves for a pair for chloride (solid line) and acetate (dashed line) ions in water. The thin dotted line is the anticipated long-range Coulomb distance dependence curve of the PMF.

with the r^{-6} and r^{-12} distance dependence. The results obtained in this study show that the use of all-repulsive potentials is qualitatively correct for pairs of like-charged as well as for pairs of charged and nonpolar side chains. However, inspection of Figure 11 shows that the PMFs fall off with the distance less rapidly than r^{-6}; the best fit is obtained when linear combinations of r^{-1}, r^{-2}, and r^{-3} terms are used. The distance dependence of the UNRES potentials for like-charged side chains should, therefore, be revised. For the charged−nonpolar solute pairs, the PMF falls off with the distance more rapidly, and use of the all-repulsive Lennard-Jones potential analogue seems to be a sufficiently good approximation. More refined treatments should also consider the appearance of shallow minima in the PMF curves; this should be particularly important for the arginine−arginine pair.

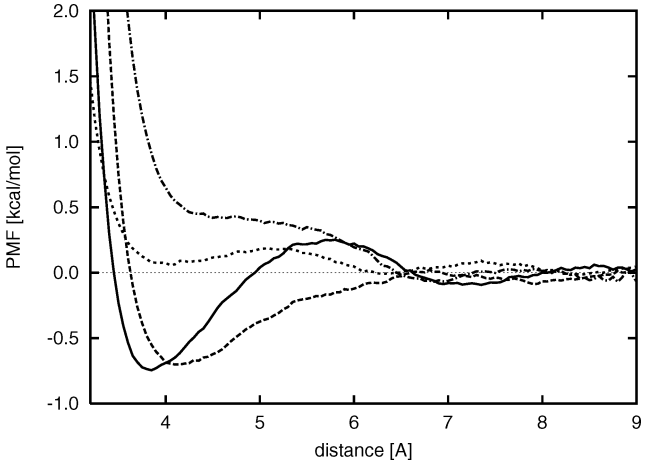

Figure 13. PMF curves for a pair for methane molecules (solid line; data from ref 14), a potassium ion and a methane molecule (dashed line), a chloride ion and a methane molecule (dot−dashed line), and an ammonium ion and a methane molecule (dotted line) in water. The thin dotted line is the zero baseline.

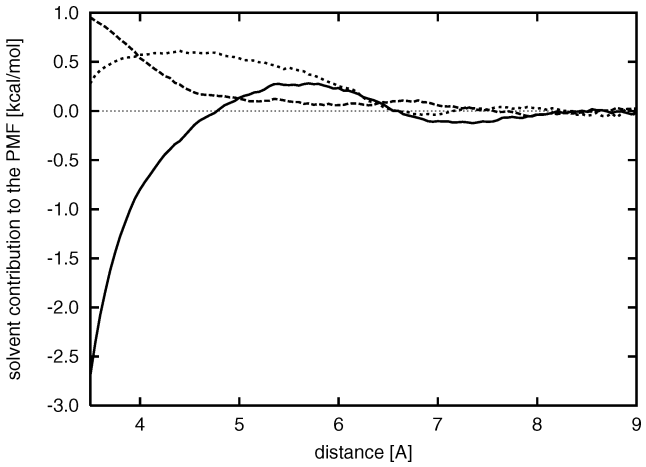

Figure 14. Solvent contribution to the PMF for a methane−methane pair (solid line), potassium−methane pair (dashed line), and chloride−methane pair (dotted line). The thin dotted line is the zero baseline.

Conclusions

The results of these studies showed that the PMF curves for pairs of simple ions in water are quite complex and possess minima even for pairs of positively or negatively charged ions. In the latter case, these minima arise from enhanced screening of each ion from its counterpart by counterions and water molecules. For more complex like-charged ions, the minima in the PMF are depleted; only in the case of a pair of guanidine ions is the minimum significant. Nevertheless, in all cases, the minimum values of the PMF are positive (taking the Coulombic distance-dependence curve with $\epsilon = 78$ as a reference PMF). This behavior shows that all-repulsive potentials used in the UNRES force field to model the interaction between like-charged side chains are probably qualitatively correct except, perhaps, for arginine. Also, in the pairs of negatively charged ions, compared to the positively charged ions, the minima are shallower or do not appear. These results are different from those of the recent study of Masunov and Lazaridis,[29] who obtained pronounced minima in the PMF curves of like-charged side chains. We have shown that the differences are caused by their using a spherical water cluster with finite size immersed in a continuous dielectric rather than the Ewald summation (which also includes summing over counterions which do not belong to the central cell) to compute electrostatic interactions. The Ewald summation, therefore, appears necessary in studying the PMFs for like-charged ions.

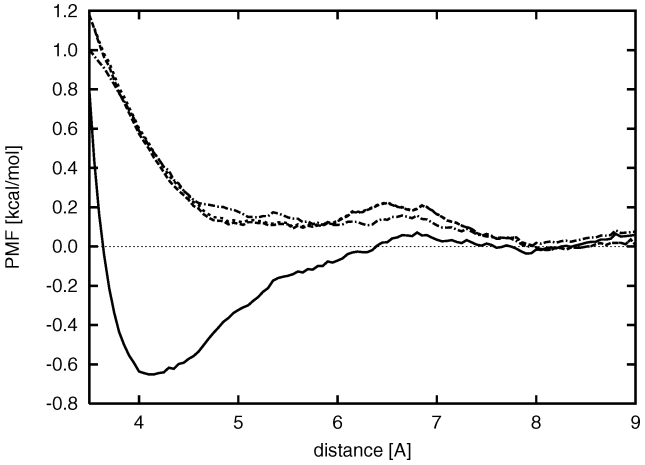

Figure 15. PMF curves and solvent contributions to the PMF obtained with two sets of methane−potassium VDW potential parameters. Solid line: total PMF obtained with the parameters derived in this work; dot−dashed line: the solvent contribution to this PMF; dashed line: total PMF obtained with the parameters determined by Åqvist;[49] dotted line: solvent contribution to that PMF. The thin dotted line is the zero baseline.

The PMF for the methane−ammonium ion pair exhibits only a minimum at 4.1 Å and the PMF for the methane−chloride pair decreases with distance until 6 Å and then exhibits only a very shallow solvent-separated minimum at 6.5 Å. This suggests that modeling of the potentials of interactions between charged and nonpolar side chains in water by all-repulsive potentials is qualitatively a good approximation.

Although the potentials for side chain interactions applied in UNRES appear to be qualitatively correct, the distance dependence appears to be more complex than the Lennard-Jones-like forms; therefore revision of the functional forms for side chain interaction potentials implemented at present in UNRES is probably needed. In the first attempt, revised formulas for the potentials can be parametrized by using the side chain pair correlation functions calculated from the data from the Protein Data Bank,[53] using the methodology developed in our earlier work.[13] This is currently being under investigation in our laboratory.

Acknowledgment. This work was supported by a grant from the Polish State Committee for Scientific Research (KBN) (7 T09A 159 21), by a grant from the National Institutes of Health (GM-14312), the National Science Foundation (MCB00-03722), and the Fogarty Foundation (TW1064). The calculations were carried out using the resources and software at (a) the Informatics Center of the Metropolitan Academic Network in Gdansk (TASK), (b) the Interdisciplinary Center of Mathematical and Computer Modeling (ICM) in Warsaw, (c) our own array of a 38-processor Pentium cluster, and (d) the National Science Foundation Terascale Computing System at the Pittsburgh Supercomputer Center.

References and Notes

(1) Kauzmann, W. Denaturation of proteins and enzymes. In *The Mechanism of Enzyme Action*; McElroy, W. D., Glass, B., Eds.; The Johns Hopkins Press: Baltimore, MD, 1954; pp 70−120.

(2) Kauzmann, W. *Adv. Protein Chem.* **1959**, *14*, 1−63.

(3) Scheraga, H. A.; Némethy, G.; Steinberg, I. Z. *J. Biol. Chem.* **1962**, *237*, 2506−2508.

(4) Poland, D. C.; Scheraga, H. A. *J. Phys. Chem*. **1965**, *69*, 2431−2442.
(5) Ben-Naim, A. *Hydrophobic interactions*; Plenum Press: New York, 1980.
(6) Ravishanker, G.; Beveridge, D. L. Theoretical studies of the hydrophobic effect. In *Theoretical chemistry of biological systems*; Náray-Szabó, G., Ed.; Elsevier: Amsterdam, 1986; Chapter 7, pp 423−494.
(7) Dill, K. A. *Biochemistry* **1990**, *29*, 7133−7155.
(8) Blokzijl, W.; Engberts, J. B. F. N. *Angew. Chem., Int. Ed. Engl*. **1993**, *32*, 1545−1579.
(9) Scheraga, H. A. *J. Biomol. Struct. Dyn*. **1998**, *16*, 447−460.
(10) Liwo, A.; Pincus, M. R.; Wawak, R. J.; Rackovsky, S.; Scheraga, H. A. *Protein Sci*. **1993**, *2*, 1697−1714.
(11) Liwo, A.; Czaplewski, C.; Pillardy, J.; Scheraga, H. A. *J. Chem. Phys*. **2001**, *115*, 2323−2347.
(12) Pillardy, J.; Czaplewski, C.; Liwo, A.; Wedemeyer, W. J.; Lee, J.; Ripoll, D. R.; Arłukowicz, P.; Ołdziej, S.; Arnautova, Y. A.; Scheraga, H. A. *J. Phys. Chem. B* **2001**, *105*, 7299−7311.
(13) Liwo, A.; Ołdziej, S.; Pincus, M. R.; Wawak, R. J.; Rackovsky, S.; Scheraga, H. A. *J. Comput. Chem*. **1997**, *18*, 849−873.
(14) Czaplewski, C.; Rodziewicz-Motowidło, S.; Liwo, A.; Ripoll, D. R.; Wawak, R. J.; Scheraga, H. A. *Protein Sci*. **2000**, *9*, 1235−1245.
(15) Czaplewski, C.; Ripoll, D. R.; Liwo, A.; Rodziewicz-Motowidło, S.; Wawak, R. J.; Scheraga, H. A. *Int. J. Quantum Chem*. **2002**, *88*, 41−55.
(16) Czaplewski, C.; Rodziewicz-Motowidło, S.; Dabal, M.; Liwo, A.; Ripoll, D. R.; Scheraga, H. A. *Biophys. Chem*. **2003**, *105*, 339−359.
(17) Pettitt, B. M.; Rossky, P. J. *J. Chem. Phys*. **1986**, *84*, 5836−5844.
(18) Buckner, J. K.; Jorgensen, W. L. *J. Am. Chem. Soc*. **1989**, *111*, 2507−2516.
(19) Dang, L. X.; Pettitt, B. M. *J. Phys. Chem*. **1990** *94*, 4303−4308.
(20) Dang, L. X.; Rice, J. E.; Kollman, P. A. *J. Chem. Phys*. **1990**, *93*, 7528−7529.
(21) Yu, H.-A.; Roux, B.; Karplus, M. *J. Chem. Phys*. **1990**, *92*, 5020−5033.
(22) Guàrdia, E.; Rey, R.; Padró, J. A. *J. Chem. Phys*. **1991**, *95*, 2823−2831.
(23) Guàrdia, E.; Rey, R.; Padró, J. A. *Chem. Phys*. **1991**, *155*, 187−195.
(24) Dang, L. X.; Pettitt, B. M.; Rossky, P. J. *J. Chem. Phys*. **1992**, *96*, 4046−4047.
(25) Karim, O. A. *J. Chem. Phys*. **1992**, *96*, 9237−9238.
(26) Friedman, R. A.; Mezei, M. *J. Chem. Phys*. **1995**, *102*, 419−426.
(27) Kovalenko, A.; Hirata, F. *J. Chem. Phys*. **2000**, *112*, 10391−10402.
(28) Kovalenko, A.; Hirata, F. *J. Chem. Phys*. **2000**, *112*, 10403−10417.
(29) Masunov, A.; Lazaridis, T. *J. Am. Chem. Soc*. **2003**, *125*, 1722−1730.
(30) Shinto, H.; Morisada, S.; Miyahara, M.; Higashitani, K. *J. Chem. Eng. Japan* **2003**, *36*, 57−65.
(31) Soetens, J.-C.; Millot, C.; Chipot, C.; Jansen, G.; Angyan, J. G.; Maigret, B. *J. Phys. Chem. B* **1997**, *101*, 10910−10917.
(32) Villarreal, M.; Montich, G. *Protein Sci*. **2002**, *11*, 2001−2009.
(33) Rozanska, X.; Chipot, C. *J. Chem. Phys*. **2000**, *112*, 9691−9694.
(34) Gaigeot, M.-P.; Borgis, D.; Staib, A. *J. Mol. Liq*. **2000**, *84*, 245−256.
(35) Torrie, G. M.; Valleau, J. P. *J. Comp. Phys*. **1997**, *23*, 187−199.
(36) Frenkel, D.; Smit, B. *Understanding molecular simulation—from algorithms to applications*; Academic Press: San Diego, CA, 1996; Chapter 7, pp 176−181.
(37) Kumar, S.; Bouzida, D.; Swendsen, R. H.; Kollman, P. A.; Rosenberg, J. M. *J. Comput. Chem*. **1992**, *13*, 1011−1021.
(38) Kumar, S.; Rosenberg, J. M.; Bouzida, D.; Swendsen, R. H.; Kollman, P. A. *J. Comput. Chem*. **1995**, *16*, 1339−1350.
(39) Pearlman, D. A.; Case, D. A.; Caldwell, J. W.; Ross, W. S.; Cheatham, T. E., III; DeBolt, S.; Ferguson, D.; Seibel, G.; Kollman, P. *Comput. Phys. Commun*. **1995**, *91*, 1−41.
(40) Case, D. A.; Pearlman, D. A.; Caldwell, J. W.; Cheatham, T. E., III; Ross, W. S.; Simmerling, C. L.; Darden, T. A.; Merz, K. M.; Stanton, R. V.; Cheng, A. L.; Vincent, J. J.; Crowley, M.; Ferguson, D. M.; Radmer, R. J.; Seibel, G. L.; Singh, U. C.; Weiner, P. K.; Kollman, P. A. *AMBER 5*; University of California, San Francisco, CA, 1997.
(41) Jorgensen, W. L.; Chandrasekhar, J.; Madura, J. D.; Impey, R. W.; Klein, M. L. *J. Chem. Phys*. **1983**, *79*, 926−935.
(42) Jorgensen, W. L.; Tirado-Rives, J. *J. Am. Chem. Soc*. **1988**, *110*, 1657−1666.
(43) Darden, T.; York, D.; Pedersen, L. *J. Chem. Phys*. **1993**, *98*, 10089−10092.
(44) Jorgensen, W. L.; Madura, J. D.; Swenson, C. J. *J. Am. Chem. Soc*. **1984**, *106*, 6638−6646.
(45) Weiner, S. J.; Kollman, P. A.; Case, D. A.; Singh, U. C.; Ghio, C.; Alagona, G.; Profeta, S., Jr.; Weiner, P. *J. Am. Chem. Soc*. **1984**, *106*, 765−784.
(46) Schmidt, M. W.; Baldridge, K. K.; Boatz, J. A.; Elbert, S. T.; Gordon, M. S.; Jensen, J. H.; Koseki, S.; Matsunaga, N.; Nguyen, K. A.; Su, S.; Windus, T. L.; Dupuis, M.; Montgomery, J. A., Jr. *J. Comput. Chem*. **1993**, *14*, 1347−1363.
(47) Bayly, C. I.; Cieplak, P.; Cornell, W. D.; Kollman, P. A. *J. Phys. Chem*. **1993**, *97*, 10269−10280.
(48) Allen, M. P.; Tildesley, D. J. *Computer Simulation of Liquids*; Clarendon Press: Oxford, U.K., 1987.
(49) Åqvist, J. *J. Phys. Chem*. **1990**, *94*, 8021−8024.
(50) Boys, S. F.; Bernardi, F. *Mol. Phys*. **1970**, *19*, 553−566.
(51) Dang, L. X.; Pettitt, B. M. *J. Am. Chem. Soc*. **1987**, *109*, 5531−5532.
(52) Magalhaes, A.; Maigret, B.; Hoflack, J.; Gomes, J. N. F.; Scheraga, H. A. *J. Protein Chem*. **1994**, *13*, 195−215.
(53) Bernstein, F. C.; Koetzle, T. F.; Williams, G. J. B.; Meyer, E. F., Jr.; Brice, M. D.; Rodgers, J. R.; Kennard, O.; Shimanouchi, T.; Tasumi, M. *J. Mol. Biol*. **1977**, *112*, 535−542.